

Direct analysis of in-line particle holograms by using wavelet transform and envelope reconstruction method

Siriwat Soontaranon¹, Joewono Widjaja¹, Toshimitsu Asakura²

¹ Institute of Science, Suranaree University of Technology, Nakhon Ratchasima 30000, Thailand

² Faculty of Engineering, Hokkai-Gakuen University, Sapporo, Hokkaido 064-0926, Japan

Abstract: We propose a new digital method for sizing particles and tracking their positions from an in-line hologram by using a combination of a wavelet transform and a reconstruction of the envelope functions. In the proposed method, the hologram is recorded by a charge-coupled device (CCD) sensor. The wavelet transform of digitized holograms gives information about the position of particles, while the reconstruction of envelope functions provides the size of particles. Preliminary theoretical and experimental verifications are presented. The system limitation of the method is discussed.

Key words: Particle holography – in-line holography – wavelet transform – digital analysis

1. Introduction

Particle sizing and tracking is one of potential applications of in-line Fraunhofer holography [1]. In in-line particle holography, opaque or semi-transparent particles are illuminated by a collimated coherent light. An interference pattern produced between light waves diffracted from the particles and the light wave transmitted directly is recorded on a light-sensitive medium such as a photographic film, and becomes a hologram. The interference pattern in the hologram contains information about both the three-dimensional (3-D) spatial position and the size of the particles which are encoded as a chirp signal and an envelope function, respectively. In a conventional analyzing method, this information is extracted by illuminating the developed hologram with the coherent light. The transmitted light reconstructs the images of the particles at the same distance as the recording distance. Since, in general, this distance is not known in advance, the image plane of best focus for each particle must be investigated by scanning the overall depth along an optical axis with

fine steps. Although this method allows us to freeze moving particles and to analyze them later, we may deal with a huge number of particles in real applications. As a consequence, the conventional reconstruction process is very tedious and time consuming.

In order to overcome this problem, Murakami [2] employed a microscope to observe directly the transmittance of the developed in-line hologram. He established a relation between the density and the diameter of interference fringes in the hologram which could provide the desired information. However, his method is applicable only to a small far-field number that corresponds to either a very big diameter of particles or a very short recording distance. As for a large far-field number, the density of fringes does not vary significantly. This leads to an inaccuracy of the method. A digital analysis of in-line holograms by means of a Wigner distribution function (WDF) was proposed by Onural and Özgen [3]. Their work was focused mainly on an extraction of the 3-D position of particles and left measurements of the particle diameter unsolved. An alternative solution for all-optical analysis of particle holograms using a wavelet transform (WT)-based correlator was proposed by Widjaja [4]. In the method, the WT is used to enhance edge features of both the images of particles reconstructed from the hologram and the image of a reference particle. By correlating these two edge-enhanced images, the position and the size of particles can be determined. Although the method is indeed useful for analyzing irregularly shaped particles, the problem in the method is that the optical system becomes complicated. Recently, the WT has also been used to extract information about the 3-D position of particles from digitally-recorded in-line holograms [5]. This method is based on an interpretation of the diffraction process as a wavelet transformation with a spherical wave for the wavelet and an axial distance of the wave propagation for its dilation (scale change). To determine the position of particles, the digital hologram is wavelet transformed by using a spherical wave-based analyzing wavelet. The position of particles can be obtained if the resultant WT gives a

Received 9 July 2002; accepted 12 October 2002.

Correspondence to: J. Widjaja
Fax: ++66-44-224185
E-mail: widjaja@ccs.sut.ac.th

maximum value. In fact, this approach is equivalent to searching the in-focus image plane of particles reconstructed from the hologram. However, since the dilation factor is determined by the axial recording distance, this method is useful only for the short axial distance. For the longer distance, the dilation increases. As a result, the admissibility condition of the wavelet is so violated that this method becomes invalid.

In the present paper, we propose a new digital method for analyzing a particle hologram by using a combination of the WT and the envelope function reconstruction. Instead of treating the diffraction process from the viewpoint of the WT, our proposed method is based on the signal processing approach applied directly to the holograms. This obviates the need for searching all depth planes. In the proposed method, the WT extracts the axial position of particles with a classical Morlet wavelet which is often used as an analyzing wavelet [6]. Here, the dilation factor is an independent variable whose value is not determined by the axial distance. A reconstruction of the envelope function is used to determine the size of particles. In comparison with the previous methods, our proposed method has the following advantages. First, it gives information about the spatial position and the size of particles. Second, since the hologram is used to extract the above information, the method is free from unwanted virtual and out-of-focus images appearing in the reconstruction process from the hologram. Third, a longer depth can be measured because the dilation factor does not depend on the axial distance. Finally, an accuracy of measurements can be maximized by taking advantage of a multi-resolution property of the WT.

2. In-line particle hologram

As for a small spherical particle with a radius of a , an amplitude transmittance of the in-line Fraunhofer hologram can be mathematically expressed as [1]

$$I(r) = 1 - \frac{2\pi a^2}{\lambda z} \sin\left(\frac{\pi r^2}{\lambda z}\right) \left[\frac{2J_1\left(\frac{2\pi ar}{\lambda z}\right)}{\frac{2\pi ar}{\lambda z}} \right] + \frac{\pi^2 a^4}{\lambda^2 z^2} \left[\frac{2J_1\left(\frac{2\pi ar}{\lambda z}\right)}{\frac{2\pi ar}{\lambda z}} \right]^2, \quad (1)$$

where λ and z are the wavelength of the illuminating light and the distance between the particle and the recording plane, respectively. r represents the radius coordinate in the hologram plane, while J_1 denotes the first-order Bessel function. The first term of eq. (1) corresponds to the directly transmitted light. The second term corresponding to a modulation of the chirp signal by an Airy function becomes very important for particle analysis, because the fre-

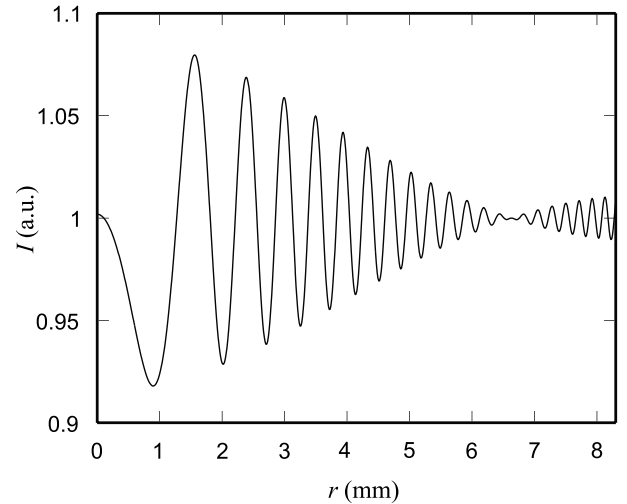


Fig. 1. Simulated in-line hologram of a spherical particle.

quency of the chirp signal is inversely proportional to the recording distance z while the minima of the Airy function are determined by the size of particles. The third term is a square of the Airy function whose amplitude is much smaller compared with the other terms [7]. Fig. 1 shows a computer plot of eq. (1), from which the above properties of three terms can be obviously observed.

3. Method

In our proposed method, the interference pattern of a hologram for a particle is captured by a CCD sensor and stored into a frame memory of the computer. Then, the captured pattern or its 1-D cross sectional profile is digitally analyzed. In digital analysis, the WT is employed to determine a space-varying frequency of the chirp signal. Since this frequency corresponds to the recording distance z , the position of the particle with respect to the recording plane can be measured. An envelope function of the interference pattern is next reconstructed in order to obtain the size of the particle. In this work, all digital computations were conducted by using the Matlab 5.3.

3.1. Wavelet transform

The WT is a mathematical technique which has been introduced in signal analysis to overcome the inability of Fourier analysis in providing local frequency spectra. The WT of a signal pattern $s(r)$ is defined as [6]

$$W(t, d) = \frac{1}{\sqrt{d}} \int_{-\infty}^{\infty} g^*\left(\frac{r-t}{d}\right) s(r) dr, \quad (2)$$

which can be considered as a cross correlation between the signal $s(r)$ and the dilated (scaled) wavelet $g(r/d)$. Here d and t are the dilation and the translation (shift) parameters, respectively. The WT is computed by dilating and translating the analyzing wavelet $g(r)$ into a set of functions having different frequency responses. By the dilation factor, unlike the WDF, the WT provides a multi-resolution decomposition of the signal in such a way that it gives a good spatial resolution at high frequency and a good frequency resolution at low frequency. When the signal $s(r)$ has the same frequency content as the dilated analyzing wavelet $g(r/d)$ in the region subtended by $g^*[(r-t)/d]$, a correlation peak is generated in the WT domain.

Fig. 2 shows the resultant WT of eq. (1) in comparison with the theoretical values. In this computation, the Morlet wavelet defined as [6]

$$g(r) = \exp(2\pi i f_0 r) \exp(-r^2/2) \quad (3)$$

was used as an analyzing wavelet with f_0 denoting the frequency of the wavelet. The vertical coordinate indicates the dilation factor, while the horizontal coordinate corresponds to the spatial position of the signal. The cross signs and the solid curve indicate the correlation peaks computed by the WT and the theoretical value of the frequency variation of the chirp signal, respectively. The correlation output is produced at any position t along the dilation d shown by the solid curve. Since the frequency is inversely proportional to the dilation [6], the result indicates that the localized frequency increases with respect to the spatial position. Therefore, the resultant WT depicted in fig. 2 agrees well with the predicted theoretical values. Furthermore, since the frequency is determined by the recording distance z , measurements of the frequency provides information about the position of particles.

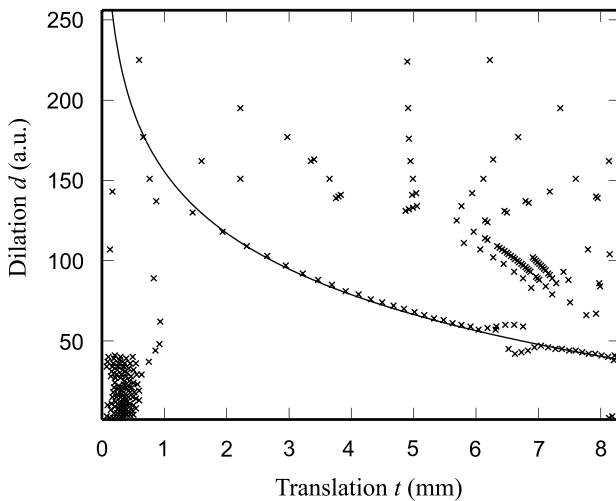


Fig. 2. Wavelet transform of eq. (1).

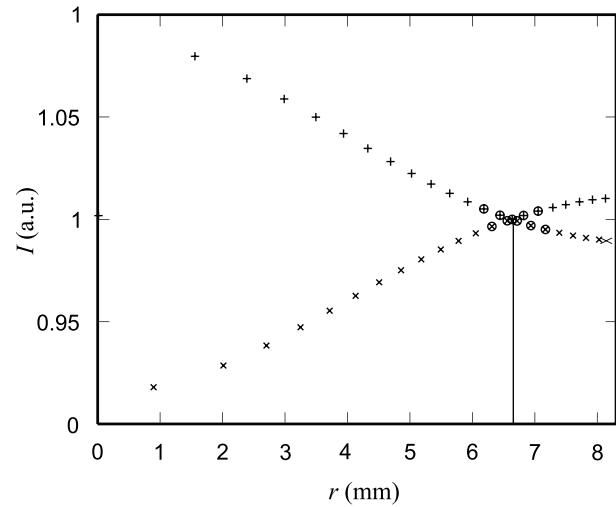


Fig. 3. Reconstruction of the Airy function and its minima.

3.2. Reconstruction of the envelope function

In order to obtain the radius of particles, a modulating function is firstly reconstructed by determining maximum and minimum amplitudes of the digitized hologram as shown in fig. 3 where the plus and the cross signs associate with the maximum and the minimum amplitudes, respectively. Second, positions of the smallest amplitude are determined by finding the smallest difference between the maximum and minimum amplitudes. The circle signs illustrated in fig. 3 show the group of pixels having the amplitude difference less than 1%. Spatial positions of these pixels are then averaged to obtain the position of the minimum of an Airy function. Since the minima are mathematically determined by an argument of the Airy function, the radius of the particle that is only an unknown value in the argument can be finally obtained.

4. Results and discussions

In a preliminary verification, the in-line hologram of an optical fiber was simulated under illumination of the coherent light operating at the wavelength of 543.5 nm. In this case, an envelope function of the interference pattern due to a line object of the fiber becomes a sinc function with the same argument [1]. By measuring the optical fiber with a microscope OLYMPUS CH30RF200, its radius was obtained to be 62.48 μm . The simulated in-line hologram was then analyzed by our proposed method. The errors of measurements for given values of the recording distance z from 15 cm to 95 cm are shown in fig. 4. Circle and cross signs correspond to the errors of measuring the distance z and the radius a , respectively. The results show that the errors in both measurements are less than 1% for a wide range of the recording distance.

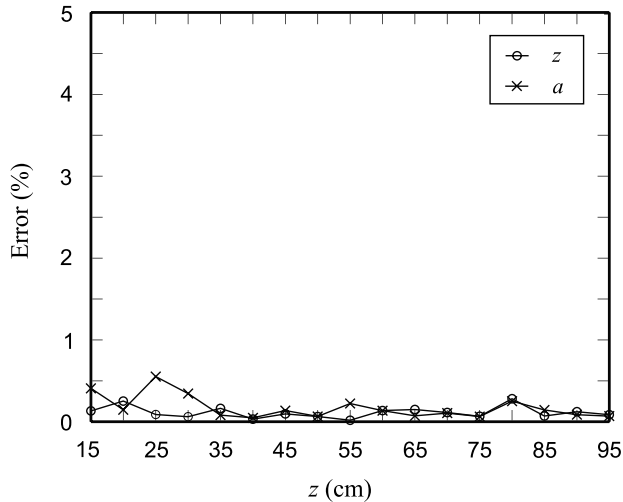


Fig. 4. Errors of measuring z and a from simulated holograms of the optical fiber.

Next, feasibility of our proposed method was experimentally verified by generating optically an in-line hologram of the optical fiber. The collimated coherent light was generated from a He-Ne laser with the wavelength of 543.5 nm. The generated hologram was recorded by using a CCD camera HAMAMATSU C5948 having the resolution of 640×480 pixels in the area of 8.3×6.3 mm. Fig. 5 shows the 1-D cross-sectional scan of the in-line hologram with three observable minima recorded at the distance $z = 30$ cm. Due to a limited experimental space, the longest distance for recording the hologram was less than that taken for the simulation. The errors of measurements using the proposed method is shown in fig. 6. The small errors of measurements for the recording distance z is in good

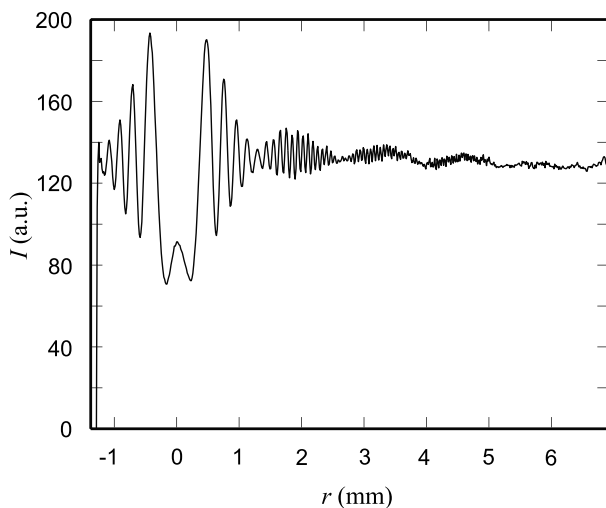


Fig. 5. In-line hologram of the optical fiber recorded at $z = 30$ cm.

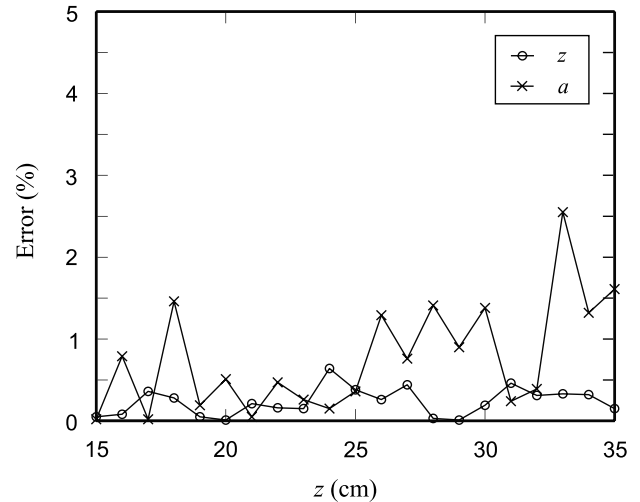


Fig. 6. Errors of measuring z and a from holograms of the optical fiber.

agreement with the simulation result. However, measurements of the particle radius a give higher errors in comparison with the simulation. The reasons for this fact may come from the following; the spatial resolution of the CCD is insufficient to sample the interference pattern and the speckle noise is overlapped over the hologram. Since the holographic signal around the minima has a very small amplitude comparable to the amplitude of the speckle noise, the determination of the minima becomes slightly difficult. This leads to a higher error of measurements.

5. System performance

A system performance of our proposed method is determined by the finite resolution and the finite aperture of the employed CCD sensor. In order to determine the combined effect of the finite resolution and the finite aperture, two requirements for measurements must be fulfilled by the CCD sensor. The first requirement is that the spatial resolution of the sensor must satisfy the Nyquist sampling theorem [8] in order to sample correctly the interference pattern. The second one is that the aperture size of the CCD must be wide enough to record the minima of the envelope function. In order to analyze the system performance we consider two major geometries of line and spherical objects. In the following discussion the CCD sensor is assumed to have a square-shaped aperture with the size of $X \times X$ and the resolution of $N \times N$ pixels. The sampling spatial frequency in either the horizontal or the vertical directions of the CCD can be mathematically expressed as

$$f_{\text{CCD}} = \frac{N-1}{X}. \quad (4)$$

5.1. Line objects

In the case of line objects, the second term of the in-line Fraunhofer hologram in eq. (1) corresponds to the chirp signal modulated by a sinc function. Since the spatial resolution of the sensor must satisfy the Nyquist sampling theorem, the relationship between the frequency of the chirp signal and the sampling frequency f_{CCD} can be expressed as

$$f_{\text{CCD}} > 2f_{\text{chirp}}. \quad (5)$$

Substitutions of the chirp frequency f_{chirp} given by $x/\lambda z$ and eq. (4) into eq. (5) give

$$x < \frac{\lambda z(N-1)}{2X}, \quad (6)$$

which describes the length of the interference pattern that can be correctly sampled by the CCD sensor placed at the distance z . Therefore, for a recording distance z , the analyzable area on the CCD is confined in the region of $0 < x < \lambda z(N-1)/(2X)$. When the recording distance becomes longer, the size of the analyzable area increases, because the longer recording distance causes the smaller frequency of the chirp signal. As a consequence, when the right term in the inequality of eq. (6) is bigger than the CCD aperture size, the range of the recorded hologram that can be analyzed becomes $0 < x \leq X$. This condition is achieved if the recording distance z is bigger than $2X^2/[\lambda(N-1)]$. We define this factor as a critical distance. In experiments, its value was approximately 39.67 cm. Therefore, the analyzable area is determined as follows

$$x < \frac{\lambda z(N-1)}{2X} \quad \text{if} \quad 0 < z \leq \frac{2X^2}{\lambda(N-1)} \quad (7a)$$

and

$$x \leq X \quad \text{if} \quad z > \frac{2X^2}{\lambda(N-1)}. \quad (7b)$$

On the other hand, in order to measure the size of the object, a minimum number of the minima n_{min} of the envelope function must be recorded by the CCD. In the case of line objects, the positions of the minima are determined by an argument of the sinc function $2ax/\lambda z$. As a result, the following relationship

$$\frac{2ax}{\lambda z} \geq n_{\text{min}} \quad (8)$$

is obtained. By substituting eqs. (7a) and (7b) into eq. (8), the smallest width of the line object that can be measured is found to be

$$a \geq \begin{cases} \frac{Xn_{\text{min}}}{N-1} & \text{if } 0 < z \leq \frac{2X^2}{\lambda(N-1)} \\ \frac{\lambda zn_{\text{min}}}{2X} & \text{if } z > \frac{2X^2}{\lambda(N-1)}. \end{cases} \quad (9)$$

Furthermore, in order to reconstruct faithfully the envelope function, a large number of interference fringes

must be present within the first minimum of the sinc function at $x = \lambda z/2a$. Since the zero of the chirp function occurs at $x = (n\lambda z)^{1/2}$ where n is the number of fringes, the number of interference fringes within the first minimum is found to be

$$n = \frac{z}{\frac{(2a)^2}{\lambda}}. \quad (10)$$

By using the far-field condition $z \gg \pi(2a)^2/\lambda$ [1], eq. (10) reduces to $n \gg \pi$ or

$$a \ll \frac{1}{2} \sqrt{\frac{\lambda z}{\pi}}. \quad (11)$$

Equation (11) describes the upper limit of the measurable object size as a function of the recording distance.

5.2. Spherical Objects

Since the chirp signal is solely determined by the axial position of the object, the analyzable area of the interference pattern for spherical objects can also be described by eqs. (7a) and (7b) with the replacement of the variable x by r . However, the positions of the minima for the Airy function and the sinc function are different. The value of the Airy function becomes minimum when the argument is 1.22π , 2.23π , 3.24π , etc. [9]. By taking this consideration into account, a minimum number of the minima n_{min} of the envelope function can be approximately described by

$$\frac{2ar}{\lambda z} \geq (n_{\text{min}} + 0.23). \quad (12)$$

To find the smallest measurable size of the spherical particle, the finite extent of the analyzable area of the interference pattern is applied. This gives

$$a \geq \begin{cases} \frac{X(n_{\text{min}} + 0.23)}{N-1} & \text{if } 0 < z \leq \frac{2X^2}{\lambda(N-1)} \\ \frac{\lambda z(n_{\text{min}} + 0.23)}{2X} & \text{if } z > \frac{2X^2}{\lambda(N-1)} \end{cases}. \quad (13)$$

By using the far-field condition to account for the number of fringes within the first minimum of the Airy function, the biggest size of the measurable particle becomes

$$a \ll \frac{1}{2} \sqrt{\frac{\lambda z}{\pi}}. \quad (14)$$

In summary, the lower limit of the measurable size for spherical objects is higher than that for line objects, while the upper limits for both objects are the same. This is due to the fact that the width between the two minima of the Airy function is wider than that of the sinc function. Fig. 7 shows the ranges of the object size and the recording distance in a logarithmic scale that can be measured by our proposed method. The ranges

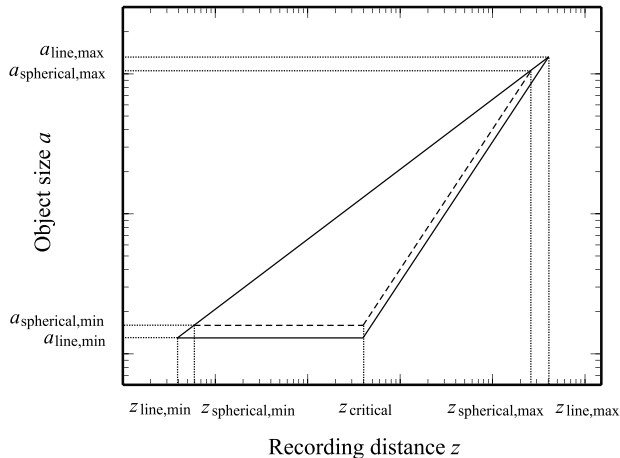


Fig. 7. Measurable size of objects and their recording distances.

of measurements for line and spherical objects are confined by the triangles drawn with the solid and the broken lines, respectively. The base and the right side of the triangle correspond to the lower limits of the measurable size of the object for the recording distances being smaller and bigger than the critical value, respectively. The left side of the triangle associates with the upper limit of the measurable size. Since the upper limits of the measurable size for both objects are the same, the two lines coincide. The maximum measurable size of the object must have a smaller value than the upper limit as described by eqs. (11) and (14). At the recording distance which is greater than the critical value, the longest recording distance and the largest size of particle could be mathematically determined by equating the maximum and the minimum values of the particle size a . In the case of line objects, this yields $z_{\text{line,max}} = X^2/\pi\lambda n_{\text{min}}^2$ and $a_{\text{line,max}} = X/2\pi n_{\text{min}}$, while for spherical particles the maximum recording distance and the maximum size are given by $z_{\text{spherical,max}} = X^2/\pi\lambda(n_{\text{min}} + 0.23)^2$ and $a_{\text{spherical,max}} = X/2\pi(n_{\text{min}} + 0.23)$, respectively. In a similar fashion, when the recording distance is smaller than the critical value, the shortest recording distance and the smallest size of line objects that can be measured becomes $z_{\text{line,min}} = 4\pi X^2 n_{\text{min}}^2/\lambda(N-1)^2$ and $a_{\text{line,min}} = Xn_{\text{min}}/(N-1)$, respectively. In the case of spherical objects we obtain $z_{\text{spherical,min}} = 4\pi X^2(n_{\text{min}} + 0.23)^2/\lambda(N-1)^2$ and $a_{\text{spherical,min}} = X(n_{\text{min}} + 0.23)/(N-1)$.

6. Conclusions

We have proposed and verified experimentally a new digital method for analyzing directly the in-line particle

holograms. A combination of the WT and the reconstruction of the envelope function are employed to extract the position of particles and their diameter from the digitized hologram, respectively. The experimental results show that the errors of measuring the particle position is less than 1% and slightly higher for errors of measuring the particle size. These results are mainly caused by the low resolution of the used CCD sensor and by the speckle noise.

We have also analyzed the dependencies of the measurable ranges of the recording distance z and the particle size a on the aperture size and the resolution of the CCD. In general, the recording distance that can be measured is much determined by the spatial resolution of the CCD sensor. To record faithfully the hologram at a short recording distance, our proposed method requires a high resolution CCD sensor. This requirement is relaxed as the recording distance becomes longer. As for the particle diameter, the smallest size that can be measured is also determined by the resolution and the diameter of the CCD. However, the upper limit depends only on the recording distance.

Acknowledgement. The authors would like to thank the Thailand Research Fund for the Royal Golden Jubilee Ph.D. Scholarship.

References

- [1] Tyler GA, Thompson BJ: Fraunhofer holography applied to particle size analysis: a reassessment. *Opt. Acta* **23** (1976) 685–700
- [2] Murakami T: A new direct analysis method for measuring particle size and location by inline hologram. *Laser Diagnostics and Modeling of Combustion*, pp. 71–76. Springer-Verlag, Berlin 1987
- [3] Onural L, Özgen MT: Extraction of three-dimensional object-location information directly from in-line holograms using Wigner analysis. *J. Opt. Soc. Am. A* **9** (1992) 252–260
- [4] Widjaja J: Automatic holographic particle sizing using wavelet-based joint transform correlator. *Optik* **107** (1998) 132–134
- [5] Buraga-Lefebvre C, Coëtmelec S, Lebrun D, Özkul C: Application of wavelet transform to hologram analysis: three-dimensional location of particles. *Opt. Lasers Eng.* **33** (2000) 409–421
- [6] Kronland-Martinet R, Morlet J, Grossmann A: Analysis of sound patterns through wavelet transforms. *Int. J. Patt. Recog. Artificial Intell.* **1** (1987) 273–302
- [7] Murata K, Fujiwara H, Asakura T: Several problems in in-line Fraunhofer holography for bubble-chamber track recording. In Robertson ER, Harvey JM (Eds.): *Proc. Conf. on Engineering Use of Holography*, pp. 289–300. University Press, Cambridge 1970
- [8] Oppenheim AV, Schaffer RW: *Discrete-time signal processing*, pp. 86–87. Prentice-Hall, New Jersey 1989
- [9] Goodman JW: *Introduction to fourier optics*. (2nd ed.), pp. 78. McGraw-Hill, USA 1996